

## A New Embedded Full Strain Components Sensor

Yann Lecieux, Cyril Lupi, Dominique Leduc, Marc François, Michel Roche

► **To cite this version:**

Yann Lecieux, Cyril Lupi, Dominique Leduc, Marc François, Michel Roche. A New Embedded Full Strain Components Sensor. Le Cam, Vincent and Mevel, Laurent and Schoefs, Franck. EWSHM - 7th European Workshop on Structural Health Monitoring, Jul 2014, Nantes, France. 2014. <hal-01021042>

**HAL Id: hal-01021042**

**<https://hal.inria.fr/hal-01021042>**

Submitted on 9 Jul 2014

**HAL** is a multi-disciplinary open access archive for the deposit and dissemination of scientific research documents, whether they are published or not. The documents may come from teaching and research institutions in France or abroad, or from public or private research centers.

L'archive ouverte pluridisciplinaire **HAL**, est destinée au dépôt et à la diffusion de documents scientifiques de niveau recherche, publiés ou non, émanant des établissements d'enseignement et de recherche français ou étrangers, des laboratoires publics ou privés.

## A NEW EMBEDDED FULL STRAIN COMPONENTS SENSOR

Yann Lecieux<sup>1</sup>, Cyril Lupi<sup>1</sup>, Dominique Leduc<sup>1</sup>, Marc François<sup>1</sup>, Michel Roche<sup>1</sup>

<sup>1</sup> GeM, CNRS UMR 6082, Université de Nantes, 2 rue de la Houssinière, 44322 Nantes

marc.francois@univ-nantes.fr

### ABSTRACT

A new concept of strain (or stress) tensor sensor is presented. Fully embedded in the structure, it measures the full 3D strain tensor while suppressing its own influence, *i.e.* allowing to find the strain (or stress) that would exist without the sensor, thanks to the Eshelby theorem. Furthermore, this theorem proves that the strain field is homogenous in the spherical (or ellipsoidal) body of the sensor, leading to perfect conditions of use for the six Bragg grating glass fibers which measure the strain of the body. After a brief overview of the theory, both mechanical and optical, we will present the results of the test performed using a prototype. This device is a simplified version of the sensor (3 channels) submitted to a hydrostatic pressure in order to assess the precision and the repeatability of the measure.

**KEYWORDS :** *mechanical sensor, embedded sensor, strain field, stress field, Bragg grating*

### INTRODUCTION

Structural health monitoring requires many kind of sensors. Among them are the strain sensors. The strain measurements are generally made onto the surface, thanks to diverse technologies (strain gages, fiber Bragg gratings, various techniques of extensometry). Surface measurements can be two dimensional, whereas available embedded strain sensors are yet limited to unidirectional measurements. Again, many technology are available. The most used are the vibrating strings, in the Civil Engineering (embedded in large concrete structure, such as dams or power plants).

SHM would gain in efficiency if a strain sensor was able to measure all together the 6 components of the strain tensor. This would make possible for example to detect directly, with the help of Von Mises criterion or Tresca's criterion, a failure at the heart of the structure. However this is not an easy task since, in general, the strain field is not uniform. This means that the strain tensor varies from one point in the structure to one another. Then, if we want to measure the full strain tensor, we must either place 6 sensors at the same point, or in positions where we are sure that the strain tensor is the same. Our sensor is based on the second solution. We propose to place 6 unidirectionnal strain sensor (fiber Bragg gratings here) along 6 different directions inside a spherical body. This peculiar geometry is chosen since Eshelby's theorem states that the strain field inside an ellipsoidal inclusion is homogeneous [1]. We are then sure that the strain tensor is the same for each sensor inside the sphere. Moreover, this theorem gives analytical relations between the strain in the inclusion and the strain that would exist in the host material in the absence of the inclusion. It is then straightforward to determine the strain in the host from the strain in the inclusion measured by the 6 sensors. Another advantage of this configuration concerns the fiber Bragg gratings. It corresponds to ideal conditions for the use of Bragg gratings [2] since it ensures the uniformity of the strain along the grating.

The aim of this paper is to demonstrate the feasibility of our concept. We will describe the sensor in the first section and then, in sections 2 to 4, explain step by step how the strain in the tested structure can be determined from the measurement of Bragg wavelength shifts. We will finally present in section 5 early experimental results obtained with a simplified 3 axes version of the sensor, designed to measure pressure.

## 1. OVERVIEW OF THE SENSOR

The sensor we propose is sketched on the figure 1a. It is a sphere made of a homogeneous material (PMMA in the present case), in which 6 optical fibers have been inserted. The directions of the fibers are aligned with the 6 normals to the faces of a dodecahedron. Each fiber is a strain sensor.

The measurement of strain with optical fiber can be performed in various ways. The measures can be distributed (Brillouin or Rayleigh scattering) or localized (Fabry-Perot sensors, fiber Bragg gratings). We choose to use fiber Bragg gratings for the ease of interrogation and to get a centimeter scale resolution.

Two technologies are possible for our sensor. In the first configuration, each fiber is placed inside a hole drilled in the sphere and glued at its extremities. The diameter of the hole is large enough so that the fiber is free to deform in the radial direction. In the second configuration, the fibers are fully embedded in the body thus the fiber is submitted to a homogeneous lateral strain due to the sensor body. In both cases, the fibers are pre-stressed at the half of their load capacity when glued, in order to avoid the buckling (or micro-buckling) when they are compressed along their axial direction. This pre-stress only shifts the resonance peak of the FBG of a constant value thus does not influence the precision of the device.

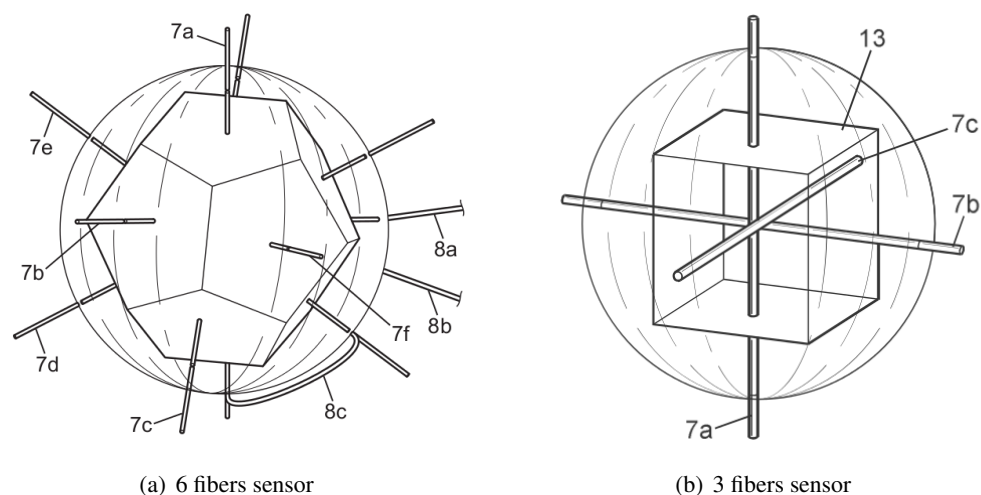


Figure 1 : Strain sensor [3]

In order to prove the feasibility of the sensor, we first made the simplified version shown on figure 1b, which contains 3 perpendicular optical fibers.

The data we experimentally measure is a shift of Bragg wavelength for the 3 or 6 (depending on the version) unidirectional sensors embedded inside the sensor body. The shifts of Bragg wavelengths are the result of the axial and radial strain that the optical fibers suffer. The Elasto-Optic theory allows to find the relationship that links the shift to the strain (see section 4). Knowing the strain of the sensor body along the direction of the fibers axis (which are exactly equal to the strain of the fibers Bragg grating), we can easily find the strain field in the sensor body by performing a matrix inversion (see section 3). The shape of the sensor is a direct application of Eshelby's theory. The spherical shape guarantees the homogeneity of the strain field inside the sensor body. Furthermore we can use Eshelby's theorem to find the strain field within the monitored structure (see section 2). Here, the spherical sensor is considered as an elastic inclusion inside the studied material. The figure 2 summarizes the steps of the calculation.

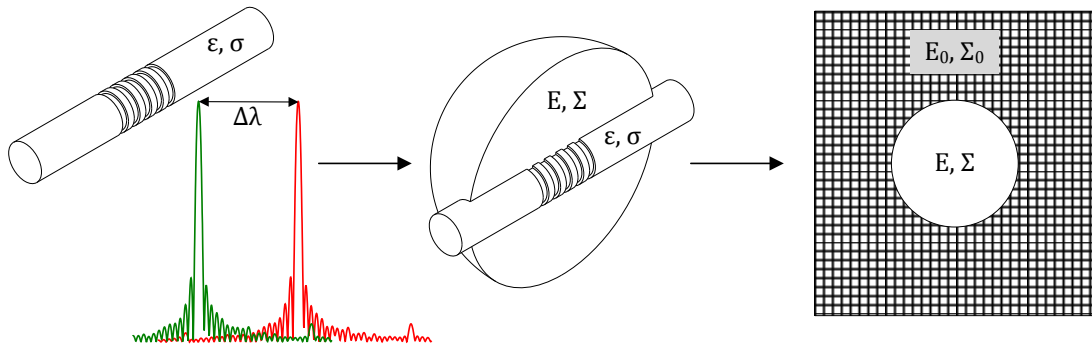


Figure 2 : Principle of the strain calculation

**2. THE RELATIONSHIP BETWEEN THE STRAIN FIELD IN THE MATRIX AND THE ONE IN THE SENSOR BODY: THE ESHELBY THEORY**

From a mechanical point of view we shall consider three phases. The strain and stress of the matrix (the values of interest) are denoted respectively by  $(\Sigma_0, E_0)$  and the strain and stress of the sensor body are denoted respectively by  $(\Sigma, E)$ . The relationship between the two is given by the localization equation :

$$E = (\mathbb{I} + \mathbb{S} : \mathbb{C}_0^{-1} : (\mathbb{C} - \mathbb{C}_0)) : E_0 \tag{1}$$

where  $\mathbb{I}$  is the fourth-rank identity tensor of components  $I_{ijkl} = (\delta_{ij}\delta_{kl} + \delta_{ik}\delta_{jl})/2$ ,  $\mathbb{C}$  and  $\mathbb{C}_0$  respectively the sensor body and the matrix elasticity tensors and  $\mathbb{S}$  the Eshelby tensor. For a sphere, its expression [1] is simply:

$$\mathbb{S} = \frac{3K_0}{3K_0 + 2\mu_0} \mathbb{P}^H + \frac{6}{5} \frac{K_0 + 2\mu_0}{3K_0 + 4\mu_0} \mathbb{P}^D \tag{2}$$

where  $\mathbb{P}^D$  and  $\mathbb{P}^H$  are respectively the deviatoric and hydrostatic projectors of expression  $\mathbb{P}_{ijkl}^H = (\delta_{ij}\delta_{kl}/3)$  and  $\mathbb{I} = \mathbb{P}^H \oplus \mathbb{P}^D$ . Finally, the constants  $(K_0, \mu_0, K, \mu)$  are respectively the bulk and shear moduli of the matrix and the sensor body. These expressions involve three points:

- In the Eshelby theory,  $E_0$  is the strain "at the infinite". It is the strain that would exist in the matrix without the sensor. This is a particularly important point for measurement.
- The strain inside the sensor body is homogeneous. Thus the fiber embedded inside will work under perfect conditions.
- From elasticity laws below, stresses are given simultaneously :

$$\Sigma = \mathbb{C} : E \tag{3}$$

$$\Sigma_0 = \mathbb{C}_0 : E_0 \tag{4}$$

One can remark that the measurement of the matrix strain  $E_0$  requires the knowledge of both the sensor and matrix elasticity tensor.

The Eshelby theory refers to a homogeneous strain state far from the inclusion (the sensor body). In the present real application, this requires a slow variation of the fields with respect to the sensor size. This is a common restriction to almost every kind of sensors.

### 3. FROM THE FIBER MEASUREMENT TO THE STRAIN ON THE SENSOR BODY

As envisaged in the final version of the sensor, we consider six fibers orientated according to the six normals of an dodecahedron. We denote as  $\vec{n}_i$  the unit vector corresponding to the direction of each fiber. Each fiber provides the deformation  $\varepsilon_i$  in the direction of its axis according to the following expression (please note that in this expression index  $i$  is not summed):

$$\varepsilon_i = \vec{n}_i \cdot E \cdot \vec{n}_i \quad (5)$$

or, equivalently:

$$\varepsilon_i = (\vec{n}_i \otimes \vec{n}_i) : E \quad (6)$$

This expression has a simple form in a convenient orthonormed tensor basis which applies (contrary to Voigt's notation) for tensor inversion:

$$\begin{aligned} B_1 &= \vec{e}_1 \otimes \vec{e}_1 \\ B_2 &= \vec{e}_2 \otimes \vec{e}_2 \\ B_3 &= \vec{e}_3 \otimes \vec{e}_3 \\ B_4 &= (\vec{e}_2 \otimes \vec{e}_3 + \vec{e}_3 \otimes \vec{e}_2) / \sqrt{2} \\ B_5 &= (\vec{e}_3 \otimes \vec{e}_1 + \vec{e}_1 \otimes \vec{e}_3) / \sqrt{2} \\ B_6 &= (\vec{e}_1 \otimes \vec{e}_2 + \vec{e}_2 \otimes \vec{e}_1) / \sqrt{2} \end{aligned} \quad (7)$$

Using formula 7 allows to gather the six equations (6) in a matrix-vector equation:

$$\varepsilon_i = N_{ij} \cdot E_j \quad (8)$$

where  $\varepsilon_i$  is the  $6 \times 1$  column matrix of the six fiber measurements.  $N_{ij}$  is the  $6 \times 6$  table composed by the six second rank tensors  $\vec{n}_i \otimes \vec{n}_i$  expressed in rows in the base  $B_j$  and  $E_j$  the  $j$ -th component of the researched strain tensor  $E$  in the same base. One can easily verify that the six normals  $\vec{n}_i$  of an icosahedron lead to an invertible matrix  $N_{ij}$  whose inverse can be computed one for all, leading to a straightforward determination of the homogenous strain  $E$  in the sensor body.

In the simplified prototype we realized, only three fibers have been embedded, along the normals of a cube (orthogonally). This device does not allow to measure the whole strain tensor, except if it is installed coaxially to the strain principal directions. It is obviously the case in the presented pressure test in which all tensors are spherical thus any direction is a principal direction. One can remark that this three-fiber device applies for the measurement of the hydrostatic pressure under any stress state, since the pressure is obtained from the trace of the stress tensor and since the trace is a mathematical invariant.

### 4. FROM THE BRAGG RESONANCE PEAK TO THE STRAIN ON THE FIBER

Fiber Bragg gratings (FBGs) are written in optical fibers by UV irradiation. An interferometric device creates fringes inside the core of the fiber. The periodic variation of the UV light intensity in the longitudinal direction induces a periodic variation of the refractive index of the core. As a consequence, the grating behaves like an interferential filter. It reflects a very narrow spectral band of the incoming light, centered on the Bragg wavelength:

$$\lambda_B = 2n_{\text{eff}}\Lambda_0 \quad (9)$$

where  $n_{\text{eff}}$  is the effective index of the mode which propagates in the core of the fiber, and  $\Lambda_0$  is the period of Bragg grating.

This behavior is a very interesting feature for sensing applications since any constraint that modifies the effective index or the period of modulation induces a shift in the Bragg wavelength. Indeed, the electric field and the electric displacement inside a material are linked by the impermeability tensor  $\mathcal{B}$  :  $\vec{E} = \mathcal{B}\vec{D}$ . The impermeability is the inverse of the permittivity tensor whose diagonal components expressed in the coordinate system of the eigen axes of the material are the square of the refractive index along these directions. When the material is deformed, the strain induces a change of impermeability (photo-elastic effect) which can be written as :

$$\Delta\mathcal{B}_{ij} = p_{ijkl}\epsilon_{kl} \quad (i, j, k, l = 1, 2, 3) \quad (10)$$

where  $p_{ijkl}$  are the components of the photo-elastic tensor and  $\epsilon_{kl}$  the components of the strain tensor  $\epsilon$ .

In the case of an optical fiber, without shear force, a first order development [4,5] of equation 10 leads to the following variation of the effective refractive index :

$$\frac{\Delta n_{\text{eff}}}{n_{\text{eff}}} = -\frac{n_{\text{eff}}^2}{2} [(p_{11} + p_{12})\epsilon_{\perp} + p_{12}\epsilon_{\ell}] \quad (11)$$

where  $\epsilon_{\perp}$  is the radial strain and  $\epsilon_{\ell}$  is the axial strain [4], which corresponds to  $\epsilon_i$  in section 3 , and the two indexes of  $p$  correspond to the expression of the tensor  $p$  in a base similar to equation 7 with  $\vec{e}_1 = \vec{n}_i$  the axial direction of the fiber.

By differentiating the equation 9, we then obtain the following shift in Bragg wavelength (in the absence of temperature variation and any other environmental parameter) :

$$\frac{\Delta\lambda_B}{\lambda_B} = -\frac{n_{\text{eff}}^2}{2} (p_{11} + p_{12})\epsilon_{\perp} + \left(1 - \frac{n_{\text{eff}}^2}{2} p_{12}\right) \epsilon_{\ell} \quad (12)$$

When the fiber is glued in two points and free to deform radially, the radial strain can be expressed as a function of the axial strain :  $\epsilon_{\perp} = -\nu\epsilon_{\ell}$ , where  $\nu$  is the Poisson ratio. The Bragg wavelength shift is then given by :

$$\frac{\Delta\lambda_B}{\lambda_B} = \left\{ 1 - \frac{n_{\text{eff}}^2}{2} [p_{12} - \nu(p_{11} + p_{12})] \right\} \epsilon_{\ell} \quad (13)$$

In this case, the measurement of Bragg wavelength shift gives directly the strain in the direction of the fiber.

### 5. TEST ON A THREE-FIBERS SENSOR UNDER FLUID PRESSURE

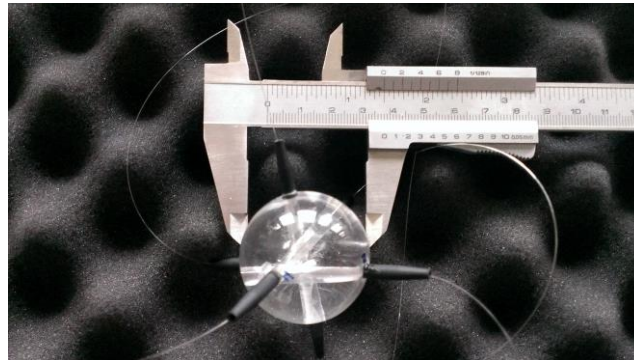


Figure 3 : The prototype

To assess the validity and the performances of the sensor, we have performed tests in a pressurized enclosure with the prototype shown on the figure 3. It is a PolyMethylMethacrylate (PMMA – or Plexiglass®) sphere of diameter 38 mm. Three optical fibers have been embedded inside, following 3 orthogonal axes. The prototype was pressured to between 0 bar and 100 bar.

The pressure and the temperature inside the enclosure has been measured using an high performance sensor (sensitivity tolerance 0.2 %, repeatability 0.05 %). The data provided by this probe are considered as the reference value. During the experiment, we have gradually increased the pressure with 10 bar increments. At each stage, we have recorded the Bragg wavelength in the 3 unidirectional sensors using a BraggMETER from Fibersensing corporation (accuracy ±2 pm). The result of this experiment is given in figure 4.

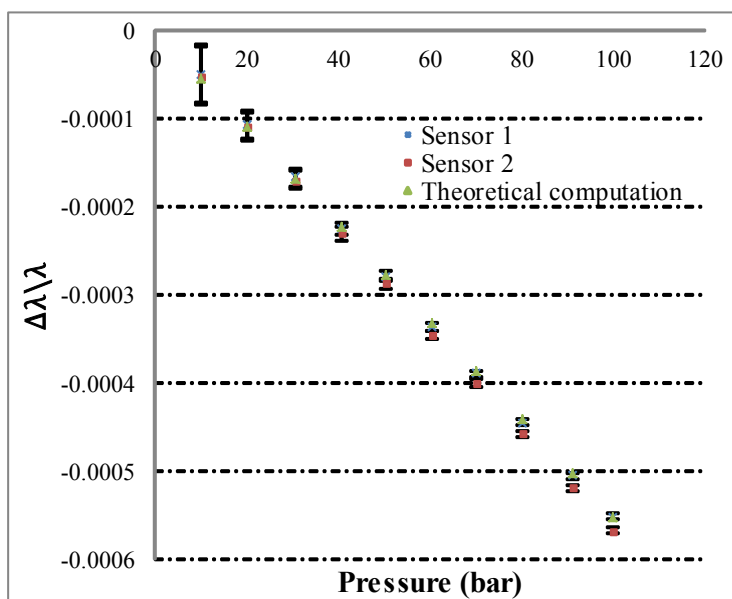


Figure 4 : Sensor performances assessment

We have then performed a linear interpolation of the data recorded for each Bragg grating. The slopes of linear regressions are given in table 1. Thus with our experimental device we obtained a sensitivity to about 1 bar. The difference between the curves is 2.7 %. Furthermore, the response of the sensor is linear. If we dont consider the two first measurement points, the maximum difference between the fitted curve and a measurement point is 2.5 % and is in average 1%.

Sensor	Sensitivity (MPa <sup>-1</sup> )	Error (%)
1	5.54e <sup>-6</sup>	2.5
2	5.69e <sup>-6</sup>	1.8
Theoretical	5.55e <sup>-6</sup>	

Table 1 : Sensitivity of the device to the pressure

For the first points, the gap is explained by the performances of the device. An accuracy of ±2 pm may induce an error of 5% on the first Bragg wavelength measurement.

We have then compared the shifts of Bragg wavelength computed analytically and determined by experiment. Knowing the pressure in the sensor (which is equal to the pressure in the enclosure),

we have computed the strain field in the sensor body. In order to compute the strain field in the optical fibers, we have again used the Eshelby theory. We consider here the glass fiber as an infinitely elongated cylinder elastic inclusion within the PMMA matrix (the sensor body). Then using formula 13, we have computed the shift of Bragg wavelength. In order to perform this analysis, we have used the values of the material coefficients given in the table 2 and the following relationship:

$$K = \frac{E}{3(1-2\nu)} , \mu = \frac{E}{2(1+\nu)} \quad (14)$$

where  $E$  and  $\nu$  are respectively the Young modulus and the Poisson ratio of the material.

Material constant	Value
$E$ (PMMA)	3.25 GPa
$\nu$ (PMMA)	0.38
$E$ (glass)	70 GPa
$\nu$ (glass)	0.17
$P_{11}$	0.113
$P_{12}$	0.252

Table 2 : Data used for the computation of the sensor theoretical measurement

The values of the material constants used are close to those given by the material supplier of Altuglas® (i.e.  $E = 3.25$  GPa and  $\nu = 0.39$ ) while the data used for the fiber glass are given in [6, 7]. We can remark that the theoretical curve is located between the experimental curves.

## 6. SOME PROSPECTS FOR THE SHM USE

Because of its size, the monitoring of civil engineering infrastructures is one of the most interesting potential applications of the sensor. It could be assembled in a network and embedded in the structure during the concrete casting. Each of these sensors would indicate the local value of the strain within the material. Measuring periodically (or better in real-time) the mechanical fields in the structure can indicate, by using adapted methods [8], the existence of a generalized or localized rigidity loss.

As a simple example, the apparition of a crack should unload the sensors close to it and due to the global equilibrium, overload sensors at different places on the structure.

The precise orientation of the fibers, as well as the location of the sensors, can be inaccurate during the structure fabrication process. However, it is possible to deduce them by minimizing the discrepancy between the computed (during the design phase) and measured (onto the new structure) fields. At last, the spherical shape leads to finite stress concentration factors thus the presence of the sensor does not involve cracking all around it. Furthermore, retaining a sensor material of same elasticity than the body would lead to no stress concentration at all.

## CONCLUSION

In this paper we presented a new strain sensor that we have recently patented [3]. This sensor consists of six fiber Bragg gratings inserted into a spherical body. According to the Eshelby theory, this sensor is able to measure the full strain tensor which would exist inside the tested structure without the sensor.

By way of illustration, and as a first test, we made a simplified version of the sensor which contains three perpendicular fibers and we used it to measure hydrostatic pressure. We then showed that the three fibers in the sensor gave identical measures to within 3% and in perfect agreement with the theory. These early results demonstrate the feasibility of the sensor. To complete this demonstration and establish its ability to measure a complex strain tensor, it remains to insert it inside an inhomogeneous material subjected to anisotropic stress.



## REFERENCES

- [1] J. D. Eshelby. The Determination of the Elastic Field of an Ellipsoidal Inclusion, and Related Problems. *Royal Society of London Proceedings Series A*, 241:376–396, August 1957.
- [2] P. A. Morvan, Y. Lecieux, D. Leduc, R. Guyard, C. Lupi and X. Chapeleau. De l'utilisation des capteurs à fibres optiques dans les matériaux composites. *Revue des composites et des matériaux avancés*, 14(2):191–205, 2014.
- [3] M. François, Y. Lecieux, D. Leduc, and C. Lupi, Patent BFF120 364GC, March, 2013.
- [4] R. Gafsi and M. A. El-Sherif. Analysis of Induced-Birefringence Effects on Fiber Bragg Gratings. *Optical Fiber Technology*, 6:299–323, July 2000.
- [5] M. S. Muller, L. Hoffmann, A. Sandmair, and A. W. Koch. Full strain tensor treatment of fiber bragg grating sensors. *Quantum Electronics, IEEE Journal of*, 45(5):547–553, 2009.
- [6] V. Bhatia. *Properties and sensing applications of long-period gratings*. PhD thesis, Virginia Tech. Blackburg, 1996.
- [7] A. Bertholds and R. Dandliker. Determination of the individual strain-optic coefficients in single-mode optical fibers. *Journal of Lightwave Technology*, 6:17, 1988.
- [8] A. Deraemaeker and G. Tondreau. Comparison of damage localization based on modal filters using strains measurements and acceleration measurements. In *IWSHM2011*, 2011.

## THANKS

We thank Ouest Valorisation SAS, which provided the financial support for the realization and the patent of the sensor.